ENSEMBLE AVERAGING IN METALLIC QUANTUM NETWORKS

FRANÇOIS MALLET*, FÉLICIEN SCHOPFER†‡, JERRY ERICSSON,
LAURENT SAMINADAYAR‡AND CHRISTOPHER BÄUERLE§
Institut Néel and Université Joseph Fourier, B.P. 166, 38042 Grenoble, France

DOMINIQUE MAILLY
Laboratoire de Photonique et Nanostructures, route de Nozay, 91460 Marcoussis, France

CHRISTOPHE TEXIER AND GILLES MONTAMBAUX
Laboratoire de Physique des Solides, Université Paris-Sud, 91405 Orsay Cedex, France

We report on the size dependence of the amplitudes of Aharonov-Bohm (AB) as well as Altshuler-Aronov-Spivak (AAS) magnetoconductance oscillations in silver networks with anisotropic aspect ratio and for various sizes ranging from 10 to 10^6 plaquettes. We show that the amplitude of both AB and AAS oscillations exhibit an unexpected dependence as a function of number of plaquettes N when the smallest dimension of the network becomes smaller than the phase coherence length: in this case, the network can be considered as a fully coherent object (mesoscopic) in one direction, whereas macroscopic in the other.

1. Introduction

The Aharonov-Bohm effect[1] in a small metallic ring is one of the most spectacular manifestation of quantum interference of electrons in a disordered conductor. By applying a magnetic flux through the ring, the conductance oscillates with a periodicity $\phi_0 = h/e$, the flux quantum, h being the Planck constant and e the charge of the electron[2]. Such magnetoconductance oscillations are a direct consequence of the coupling of the electron charge to the vector potential, and is thus the most direct evidence of the quantum nature of the conduction in mesoscopic systems[3].

An important point is the understanding of how such quantum effects disappear when going from mesoscopic to macroscopic conductors[4]. If one considers lines of N mesoscopic metallic rings, the Aharonov-Bohm (AB) conductance oscillations

*Present address: Service de Physique de l'État Condensé, DSM/DRECAM/SPEC, CEA Saclay, Orme des Merisiers, 91191 Gif-sur-Yvette cedex, France.
†Present address: Laboratoire National de Métrologie et d'Essais, 29 avenue Roger Hennequin, 78197 Trappes, France.
‡Member of the Institut Universitaire de France, 103 boulevard Saint Michel, 75005 Paris, France.
§This work is supported by ACI grants # 02 2 0222 and # NN/02 2 0112, and the European Commission FP6 NMP-3 project 505457-1 Ultra-1D. Mail to: quspin@grenoble.cnrs.fr.

$\delta G_{\rm AB}/G$ vanishes to zero as $1/\sqrt{N}$. This has been demonstrated in a pioneering experiment by Umbach el al.[5] where they studied lines of N silver rings with N varying from 1 to 30. The authors showed that the amplitude of the AB oscillations decrease when increasing the number of rings N.

On the other hand, there exist a second class of magnetoconductance oscillations. They are due to interferences between time reversed trajectories and therefore *do* survive such an ensemble averaging. These oscillations have a period of $\phi_0/2$[6,7] and are known as Altshuler-Aronov-Spivak (AAS) oscillations. The robustness of these oscillations has been shown in several experiments [5,8,9].

We would like to stress that all these experiments have been carried out in a regime where the phase coherence length L_ϕ is much smaller than the system size. One then deals with the simple case of an ensemble averaging consisting in a summation of *uncorrelated* contributions from phase coherent regions. In what follows, we will address the issue of ensemble averaging when the system size decreases and becomes of the order or smaller than the phase coherence length L_ϕ.

2. Sample Fabrication

Samples are fabricated on a silicon substrate using electron beam lithography on polymethyl-methacrylate resist. Silver is deposited from a 99.9999 % purity source using an electron gun evaporator and lift-off technique without any additional adherence layer. All samples have been evaporated in a single run to ensure that the sample characteristics (elastic mean free path $l_e \approx 15\,nm$ and phase coherence length L_ϕ) are similar.

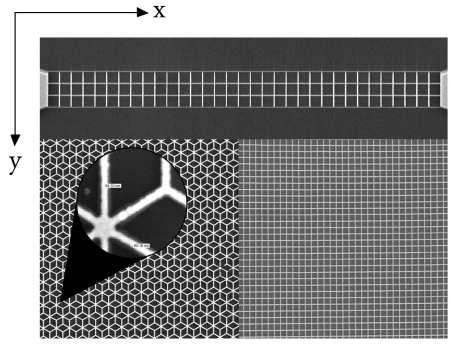

Figure 1. Scanning Electron Micrograph of several samples of various sizes; two contacts are visible for the small sample.

In this work, two different topologies have been studied: the square lattice and the so-called $\mathcal{T}_3$ lattice[10]. The wires forming the networks are $60\,nm$ wide, $50\,nm$ thick and $640\,nm$ ($690\,nm$) long for the square ($\mathcal{T}_3$) lattice. The size of the plaquettes (square or diamond) is chosen such that the magnetic field corresponding to one flux quantum ϕ_0 per plaquette is $B = 100\,G$. All networks with number of plaquettes N

varying from 10 to 10^6 have the same aspect ratio $L_x/L_y = 10$ (see figure 1). As a consequence, their resistances are similar and of the order of $100\,\Omega$. Measurements have been performed at a temperature of $400\,mK$ at which the signal to noise ratio is optimum. At this temperature, the phase coherence length, determined from standard weak localization measurements on a wire fabricated on the same wafer is about $L_\phi \simeq 6\,\mu m$[11].

3. Experimental Results and Discussion

In figure 2a we show typical data for the magnetoresistance of a square network with 3000 plaquettes at low fields. Clear magnetoconductance oscillations are observed around zero field. These oscillations have a period of $B = 50\,G$, as emphasized in the Fourier spectrum (figures 2b), which corrsponds to $\phi_0/2$ per plaquette and are identified as the AAS oscillations.

At fields typically higher than the field which suppresses weak localization, we observe a different type of oscillations. They are shown in figure 3 for networks with different number of plaquettes as well as their Fourier spectra. These oscillations have a periodicity of $B = 100\,G$ and correspond to AB oscillations.

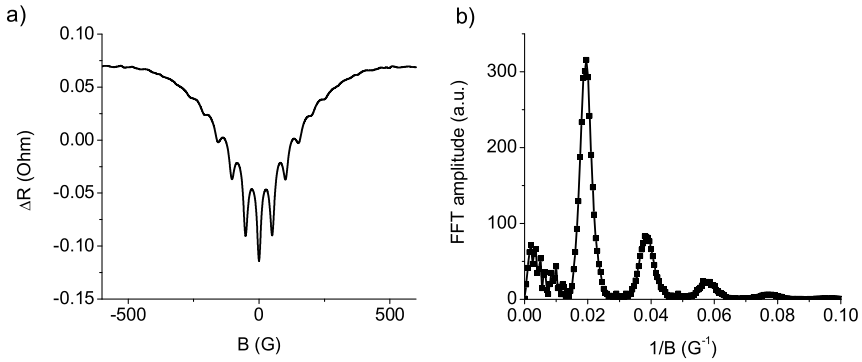

Figure 2. Magnetoresistance of a square network containing 3000 plaquettes at low field data and its Fourier amplitude.

Let us now look at the size dependence of the AB as well as AAS oscillations *versus* the number of plaquettes N. To measure the AB oscillations we sweep the magnetic field from $7000\,G$ to $13000\,G$, whereas for the AAS oscillations we cover a field range of $\pm 1200\,G$. The amplitude of the AB oscillation is obtained by integration of the 1st peak of the Fourier spectrum of the magneto resistance curve. The AAS amplitude is obtained in a similar way. Note however, that the second harmonic ($\phi_0/2$) of the AB oscillation has the same frequency as the first harmonic ($\phi_0/2$) of the AAS oscillation. For small networks (typically $N \leq 100$) this contribution cannot be completely neglected. In order to extract the AAS signal, we therefore determine first the amplitude of the second harmonic of the AB

oscillations at high field and then subtract this amplitude from the first harmonic of the oscillations measured at low field.

In Figure 4 we display the amplitude of magnetoconductance oscillations (AAS and AB) extracted from the Fourier spectra as a function of the number N of plaquettes for both, square and $\mathcal{T}_3$ lattices. For large networks ($N \gtrsim 300$), the amplitude of the AB oscillations clearly decreases as $1/\sqrt{N}$, whereas the amplitude of the AAS oscillations are independent on the number of plaquettes as naively expected.

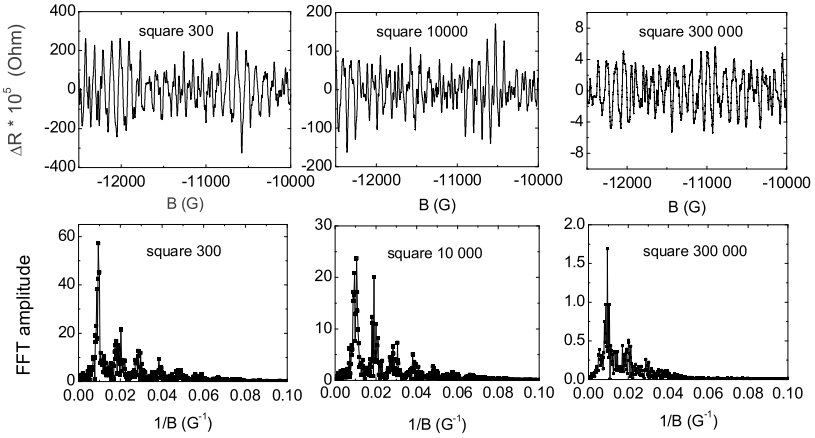

Figure 3. Magnetoresistance for several networks at high magnetic fields as well as their Fourier spectra. The average resistance is $\approx 100\,\Omega$ for the three samples.

More surprising is the behavior observed for small networks: when they contain typically less than $N \simeq 300$ plaquettes, the amplitude of the AB oscillations varies faster than $1/\sqrt{N}$. At the same time the AAS amplitude now depends on N (figure 4). In the following, we will show that this new behavior results from a dimensional crossover when the transverse size of the network becomes smaller than the phase coherence length, a new regime where the transport properties are effectively one-dimensional on the two-dimensional network. For our discussion we start with the following equation which relates the AAS conductance oscillation $\Delta g_{\rm AAS}$ and the AB conductance oscillation $\delta g_{\rm AB}$[12,13,14,15].

$$\delta g_{\rm AB}^2 = \frac{2\pi L_T^2}{3L_x^2}\Delta g_{\rm AAS} \tag{1}$$

where L_T is the thermal length and L_ϕ the phase coherence length. As we are working at constant temperature, both quantities are fixed parameters. In the following we consider a network of dimensions $L_x \times L_y$ (see figure 1). Note however, that experiments presented here are performed on several networks of different sizes,

but *of constant aspect ratio* $L_x/L_y = 10$. The length and width of the networks thus scale with the number of plaquettes N as $L_x = 10L_y \propto \sqrt{N}$.

Let us first consider large networks with both dimensions larger than the phase coherence length: L_x, $L_y \gg L_\phi$. In this case the weak localisation correction $\Delta\sigma$ which is directly related to the AAS oscillation is size independent as interfering time reversed trajectories extend over a typical size L_ϕ and therefore do not feel the boundaries of the system. The AAS amplitude varies as $\Delta g_{\rm AAS} \propto L_y/L_x$ and is hence is independent on N:

$$\Delta g_{\rm AAS} \propto N^0 \tag{2}$$

In this regime we also see from eq. (1) that $\delta g^2_{\rm AB} \propto L_y/L_x^3$, which leads to:

$$\delta g_{\rm AB} \propto N^{-1/2} \tag{3}$$

This is exactly what is observed for large networks: when the number of plaquettes is larger than $\simeq 300$, electrons diffuse on what they feel as a two-dimensional network.

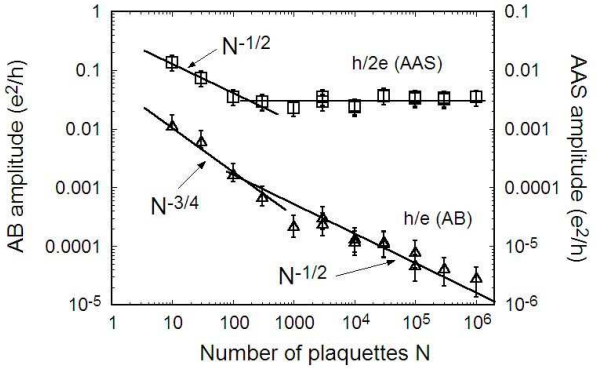

Figure 4. AAS amplitude $\Delta g_{\rm AAS}$ (□) and AB amplitude $\delta g_{\rm AB}$ (△) as a function of the number of plaquettes N for different networks of various sizes.

For smaller networks, the transverse dimension L_y eventually becomes smaller than the phase coherence length: we enter a regime where the network becomes transversally coherent whereas it remains longitudinally incoherent: $L_y \ll L_\phi \ll L_x$. In this case, we have the usual quasi-1D scaling $\Delta\sigma_{\rm AAS} \propto L_\phi/L_y$. Therefore we find $\Delta g_{\rm AAS} \propto 1/L_x$ and $\delta g^2_{\rm AB} \propto 1/L_x^3$, which leads to:

$$\Delta g_{\rm AAS} \propto N^{-1/2} \tag{4}$$

$$\delta g_{\rm AB} \propto N^{-3/4} \tag{5}$$

Indeed, this is exactly what is observed for small networks (see figure 4). The crossover hence appears when the phase coherence length is of the order of the smallest extension of the network. In our case it occurs at a network size of $N \simeq 300$ which corresponds to $L_y \simeq 3.8\,\mu m$. This length has to be compared with the phase

coherence length $L_\phi \simeq 6\,\mu m$ measured at $T = 400\,mK$ on a wire fabricated on the same wafer. This is in relatively good agreement and hence supports our analysis.

Finally let us compare these N dependences with the case of a $1D$ chain where the number N of rings scales linearly with the length L_x of the chain. In this case we have $\delta g^2_{\rm AB} \propto 1/L_x^3 \propto 1/N^3$ and $\Delta g_{\rm AAS} \propto 1/N$. Since the conductance g scales as $1/N$, this yields for the relative fluctuations $\Delta g_{\rm AAS}/g \propto N^0$ and $\delta g_{\rm AB}/g \propto 1/\sqrt{N}$ as was observed experimentally[5].

4. Conclusions

In conclusion, we have measured both Aharonov-Bohm ϕ_0 periodic oscillations and Altshuler-Aronov-Spivak $\phi_0/2$ periodic oscillations in metallic networks containing 10 to 10^6 plaquettes. Ensemble averaging leads to different size dependences for small and large networks. The crossover takes place when the width of the network is of the order of the phase coherence length; this behavior does correspond to a dimensional crossover between effectively one- and two-dimensional networks. In this new regime, we have shown that the amplitude of the AB oscillations varies as $N^{-3/4}$ and the AAS oscillations as $N^{-1/2}$, a behavior which has never been observed up to now.

References

†. Present address: Bureau National de Métrologie, Laboratoire National d'Essais, 29 avenue Roger Hennequin, 78197 Trappes, France.
1. Y. Aharonov and D. Bohm, Phys. Rev. **115**, 485 (1959).
2. Y. Gefen, Y. Imry, and M. Ya. Azbel, Phys. Rev. Lett. **52**, 129 (1984); M. Büttiker, Y. Imry, and M. Ya. Azbel, Phys. Rev. A **30**, 1982 (1984).
3. S. Washburn and R. A. Webb, Adv. Phys. **35**, 375 (1986).
4. F. Schopfer, F. Mallet, D. Mailly, C. Texier, G. Montambaux, C. Bäuerle and L. Saminadayar, Phys. Rev. Lett. **98**, 026807 (2007).
5. C. P. Umbach, C. Van Haesendonck, R. B. Laibowitz, S. Washburn, and R. A. Webb, Phys. Rev. Lett. **56**, 386 (1986).
6. B. L. Al'tshuler, A. G. Aronov, and B. A. Spivak, JETP Lett. **33**, 94 (1981).
7. D. Yu. Sharvin and Yu. V. Sharvin, JETP Lett. **34**, 272 (1981).
8. B. Pannetier, J. Chaussy, R. Rammal, and P. Gandit, Phys. Rev. Lett. **53**, 718 (1984); B. Douçot and R. Rammal, Phys. Rev. Lett. **55**, 1148 (1985).
9. G. J. Dolan, J. C. Licini, and D. J. Bishop, Phys. Rev. Lett. **56**, 1493 (1986).
10. J. Vidal, R. Mosseri, and B. Douçot, Phys. Rev. Lett. **81**, 5888 (1998); C. Naud, G. Faini, and D. Mailly, Phys. Rev. Lett. **86**, 5104 (2001).
11. F. Mallet, F. Schopfer, D. Mailly, C. Texier, G. Montambaux, C. Bäuerle, and L. Saminadayar, to be published.
12. I. L. Aleiner and Ya. M. Blanter, Phys. Rev. B **65**, 115317 (2002).
13. T. Ludwig and A. D. Mirlin, Phys. Rev. B **69**, 193306 (2004).
14. C. Texier and G. Montambaux, Phys. Rev. B **72**, 115327 (2005).
15. É. Akkermans and G. Montambaux, *Physique mésoscopique des électrons et des photons*, EDP Sciences (2004); *Mesoscopic physics of electrons and photons*, Cambridge University Press, Cambridge (2007).